View metadata, citation and similar papers at core.ac.uk
brought to you by CORE
provided by NASA Technical Reports Server

General Disclaimer

One or more of the Following Statements may affect this Document

- This document has been reproduced from the best copy furnished by the organizational source. It is being released in the interest of making available as much information as possible.

- This document may contain data, which exceeds the sheet parameters. It was furnished in this condition by the organizational source and is the best copy available.

- This document may contain tone-on-tone or color graphs, charts and/or pictures, which have been reproduced in black and white.

- This document is paginated as submitted by the original source.

- Portions of this document are not fully legible due to the historical nature of some of the material. However, it is the best reproduction available from the original submission.

Produced by the NASA Center for Aerospace Information (CASI)

INVESTIGATION OF LASER DYNAMICS, MODULATION AND CONTROL

BY MEANS OF INTRA-CAVITY TIME VARYING PERTURBATION

under the direction of

S. E. Harris

Quarterly Status Report

(Report No. 9)

for

NASA Grant NGL-05-020-103

National Aeronautics and Space Administration

Washington, D. C.

for the period

1 November 1969 - 31 January 1970

M. L. Report No. 1831

February 1970

Microwave Laboratory
W. W. Hansen Laboratories of Physics
Stanford University
Stanford, California

N70-20759 (ACCESSION NUMBER)
22 (PAGES)
CR-108287 (NASA CR OR TMX OR AD NUMBER)
1 (THRU)
(CODE)
16 (CATEGORY)
FACILITY FORM 602

MAR 1970
RECEIVED
NASA STI FACILITY
INPUT BRANCH

STAFF

NASA Grant NGL-05-020-103

for the period

1 November 1969 — 31 January 1970

PRINCIPAL INVESTIGATOR

S. E. Harris

PROFESSORS

A. E. Siegman

R. L. Byer

RESEARCH ASSISTANTS

J. E. Murray

J. Falk

D. J. Taylor

S. C. Wang

INTRODUCTION

The work under this Grant is generally concerned with the generation, control, and stabilization of optical frequency radiation. In particular, we are concerned with obtaining tunable optical sources by means of non-linear optical techniques. During this period work was active in the following areas. These were: first, pulse lengthening via overcoupled internal second harmonic generation; second, electronic tuning and short pulsing of dye lasers; third, laser stabilization studies; and fourth, backward wave oscillation. Progress reports on these topics are given in the following sections.

During this period the following publications have been submitted for publication and/or have been published:

S. E. Harris, "Tunable Optical Parametric Oscillators," submitted to Proc. IEEE.

S. E. Harris, S. T. K. Nieh, and D. K. Winslow, "Electronically Tunable Acousto-Optic Filter," submitted to Applied Physics Letters.

1. <u>Pulse Lengthening Via Overcoupled Internal Second Harmonic Generation</u> (S.E. Harris and J.E. Murray).

Since our applications for pulse lengthening require substantial pulse energies, an analysis has been done to determine how the available energy divides between the fundamental and second harmonic. Also, preliminary experimental data have been obtained which indicate substantial pulse lengthening for fundamental frequency output.

The determination of the energy relationships for this pulse lengthening process begin with the normalized rate equations presented previously.

$$\frac{dn}{dt} = -\varphi n$$

$$\frac{d\varphi}{dt} = \varphi(n - 1) - \beta\varphi^2 ,$$

where φ and n are normalized photon density and population inversion respectively, and β is the normalized coupling parameter to the second harmonic. (Precise definitions of these variables were given in the previous report.) From these equations it is apparent that the number of fundamental photons lost to second harmonic generation is given by

$$\int_{T_0}^{T_f} \beta\varphi^2 \, dT ,$$

where T_0 and T_f are initial and final times for the Q-switched pulse. Using the first rate equation, the variable of integration can be changed to n , giving the following expression for the second harmonic energy:

$$E_{SH} = \left(\frac{h\nu}{2} N_0\right) \beta \int_{n_f}^{n_0} \varphi \, dn \quad ,$$

where n_0 and n_f are the initial and final values for the normalized population inversions and the relation in front is the normalizing constant for a three-level laser system. (For a four-level laser system the two in the denominator is not present.) Using the solution for φ previously presented, this integral can be carried out, giving an analytic expression for the second harmonic energy in terms of n_0 and β .

Figure 1 shows this result for $\beta \gg 1$ and at constant pump power. The ordinate is normalized to the total energy stored in the initial inversion. Since the pumping level is held constant, the normalized inversion n_0 is varied by changing the single pass loss at the fundamental. The relationship between the two is:

$$n_0 = - N_0 \frac{\sigma}{A} \ln(1 - \alpha) \quad ,$$

where N_0 is the initial population difference between the energy levels of the laser transition and is dependent on pumping power; σ and A are the laser transition cross-section and the area of the laser mode in the lasing material; and α is all single pass losses at the fundamental except those due to second harmonic generation. The dashed curve indicates that fraction of the energy stored in the initial inversion which is available for laser action, i.e., the difference between the initial and final population inversions. For large values of β as for this figure, it is the difference between the initial stored energy and that energy required for theshold. For values of β near one or less, the final population inversion drops appreciably below that required for threshold, shifting these curves slightly to

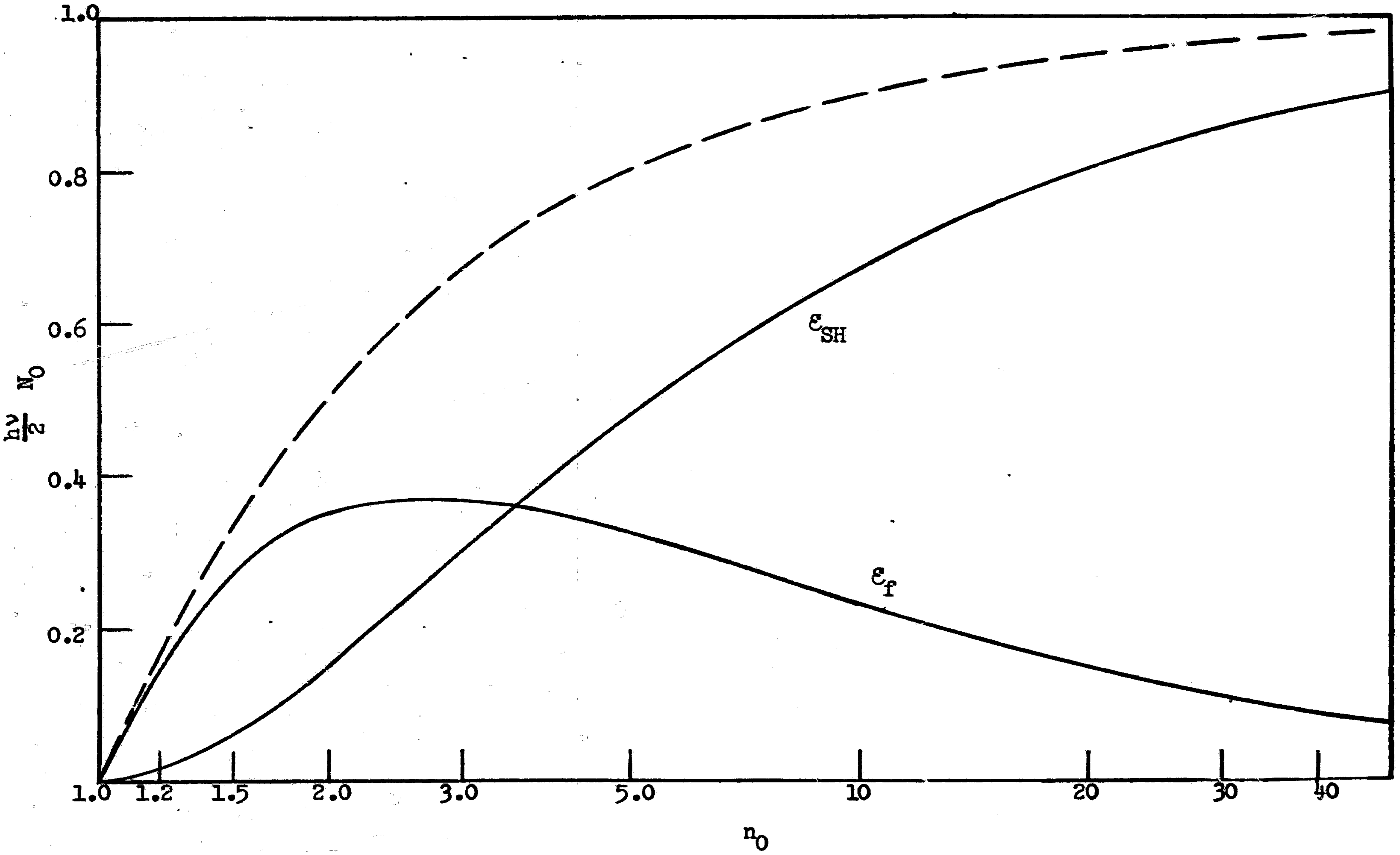

FIG. 1--Second harmonic and fundamental energies versus normalized initial inversion at constant pumping power and for $\beta \gg 1$. The dashed curve indicates the total energy available for laser action.

the left relative to n_0 . Also shown in Fig. 1 is the fraction of the total energy dissipated at the fundamental; it is the difference between the available and second harmonic energies.

Three interesting features are brought out by this analysis. First, at the expense of energy efficiency, lengthened fundamental pulses can be obtained from this pulse lengthening scheme. The maximum in the $\mathcal{E}_f$ curve occurs at

$$n_0 = \frac{\beta - 1}{\beta} e \quad ,$$

where $e = 2.718...$. The optimum single pass loss is then

$$\alpha = 1 - \exp\left[\frac{N_0 \sigma \beta}{A(\beta - 1)e}\right] \quad .$$

The fraction of $\mathcal{E}_f$ which is useful output at the fundamental is the ratio of the output coupling loss to the total loss. The maximum ratio of fundamental to stored energy, however, is given by

$$\mathcal{E}_f = \frac{\beta}{(\beta - 1)e} \quad .$$

For large values of β , as are required for pulse lengthening, this reduces to 36.8% of the energy stored in the initial inversion.

A second result is that, since the analysis is completely independent of the nature of the square law loss used to achieve lengthening, it applies equally well to all such pulse lengthening schemes. Therefore, in cases where the square law loss mechanism does not give rise to useful output, the maximum energy output of the system is only 37% of the energy stored in the initial inversion. In contrast, the energy taken from the fundamental by the square law loss approaches 100% with large values of n_0 . For our lengthening scheme, this energy appears as second harmonic output.

Thirdly, it turns out that these energy relations are independent of β for $\beta \gg 1$; therefore pulse lengthening can be accomplished at constant pulse energy for either fundamental or second harmonic outputs.

Experimental Results

We have had some success from preliminary experiments demonstrating this pulse lengthening scheme. As indicated previously, we are using a ruby laser system with KDP as the second harmonic crystal. The maximum value of β for this system, which was reported last time, was based on the criteria

$$w = \sqrt{2}\,\rho\,\ell \quad ,$$

which determines the beam radius, w in terms of the walk-off angle ρ, and crystal length ℓ . For crystal lengths in excess of a few millimeters, this criteria is overly conservative. Based on the work of Boyd and Kleinman,[1] β's in excess of a thousand should be obtainable. Although the cross-section of the second harmonic mode will be asymmetric due to walk-off in the KDP for these large values of β , the TEM_{oo} nature of the beam will not vary inasmuch as the fundamental remains TEM_{oo}.

The experimental effort has been divided into two parts, one to demonstrate appreciable energies and pulse lengthening at the second harmonic and the other to do the same at the fundamental. Since the experiment at the fundamental is somewhat easier and there is less

[1] Boyd and Kleinman, J. Appl. Phys. 39, 8597 (1968).

danger of damage to the second harmonic crystal, it was attempted first.

Figure 2 is a schematic of the arrangement of cavity components for this experiment at the fundamental. Mirror M_1 has a 60 cm radius with a dielectric coating for maximum reflectivity at 0.694 μ; M_2 was a sapphire etalon with a maximum reflectivity of 26.1%. The electro-optic Q-switch and polarizer were misaligned with the cavity axis to prevent spurious resonances which could have led to an unstable threshold condition. The ruby rod and second harmonic generator (SHG) were cut at Brewster's angle. The polarizer was the beam splitting model of the Glan-Kappa type. It was utilized to protect the ruby from the second harmonic radiation. The SHG was located as close as possible to M_2 and the ruby rod as close as possible to M_1. This minimized the mode size in the SHG and maximized it in the ruby rod to give the maximum β for a given mirror spacing. The aperture was very important to prevent the laser from breaking into higher order modes. Since all higher order modes have a smaller effective β for a given configuration, they see less loss to the SHG. Thus the laser will tend to switch to higher order modes as the oscillation builds up unless prevented by the aperture. Pulse waveforms were monitored with an hpa 4204 photo-diode and a TEK 519 oscilloscope. Pulse energies were measured with a TRG thermopile.

Figure 3 shows data obtained at constant pumping power and relatively low output energy. The dashed lines represent the best fits to the experimental points. The data with β's of 150 or less were obtained with an effective mirror spacing of 55 cm by tuning the crystal with angle. The data with β's of 200 and 450 were obtained with mirror spacings of 57 and 58.5 cm. The SHG was not tuned with angle at these spacings to avoid the possibility of damage to the SHG due to small mode sizes and the high

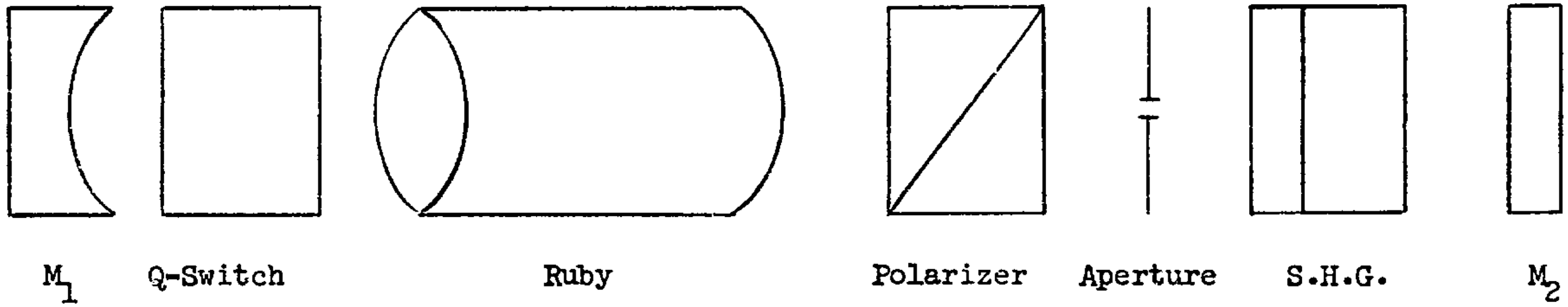

FIG. 2--Schematic diagram of laser cavity components for the experiment to lengthen fundamental frequency pulses.

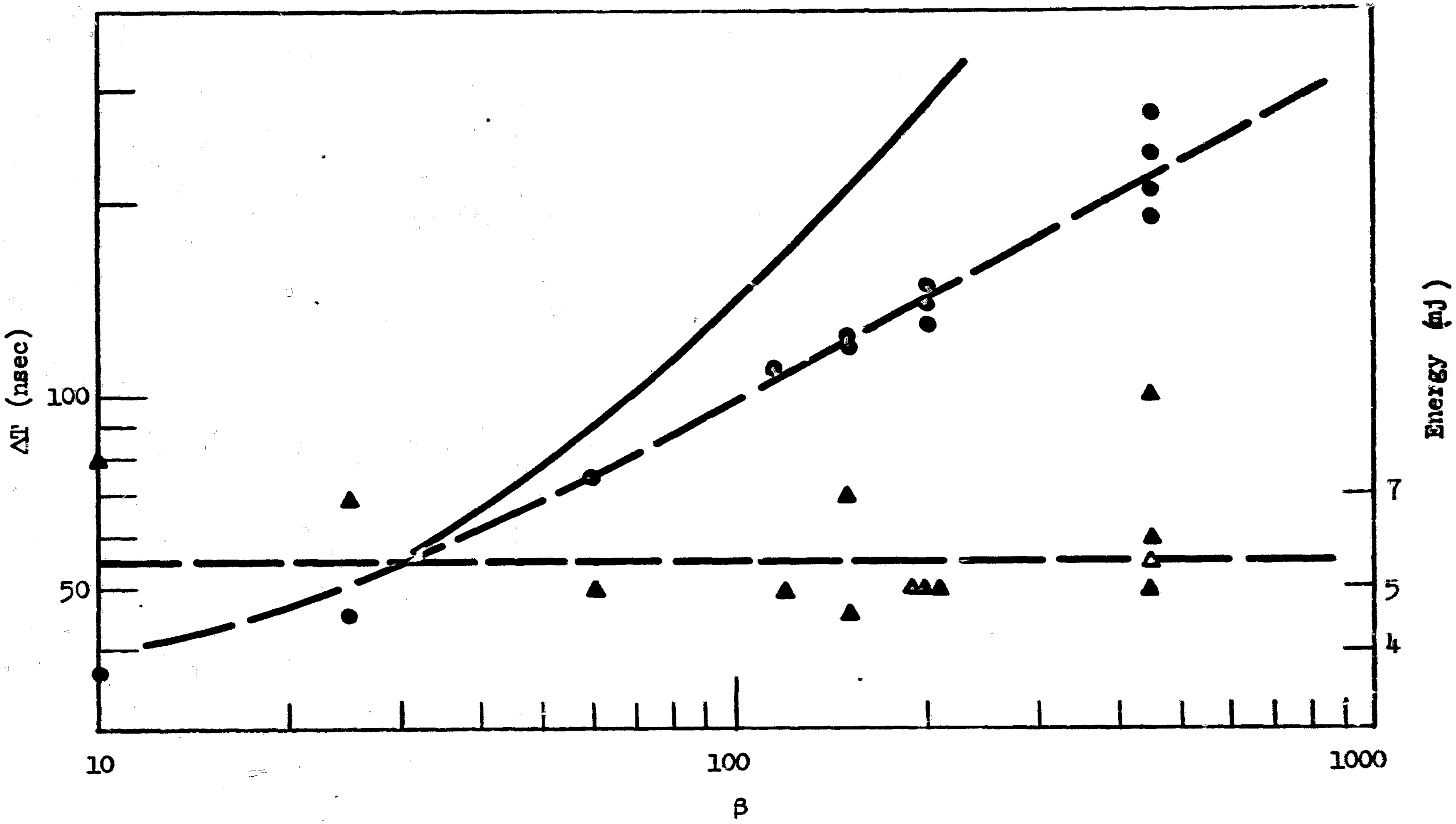

FIG. 3--Pulse length and energy versus β for the fundamental at constant pumping power. Experimentally obtained pulse lengths are indicated by the small circles, their energies by the triangles. The dashed lines represent approximate fits to the experimental points. The solid line is a theoretical prediction of pulse length versus β based on the data point with β = 10 .

peak powers of unlengthened Q-switched pulses. The solid line shows the theoretical prediction of pulse length versus β , based on the 37 nsec pulse with a β of 10. It shows that the effective β's obtained experimentally were considerably less than those calculated from the geometry and crystal parameters. The most probable source of error is the estimation of mode size at the SHG and ruby.

In addition to this data, pulses were obtained in the 12 - 16 mj range with half-amplitude widths between 250 and 400 nsec. At higher energies, the pulse waveform became irregular. This seemed to be correlated with the laser breaking into higher order modes. A change in the aperture spacing or position might allow higher pulse energies in the future.

During the next quarter, we hope to obtain the same type of experimental data for second harmonic pulses, and possibly to improve on the data for fundamental pulses.

2. Electronic Tuning and Short Pulsing of Dye Lasers (D. J. Taylor)

The goal of this project is to obtain an electronically tunable coherent light source by inserting a straight-through acousto-optic filter element into the cavity of a dye laser. The dye cell may be considered to be a constant gain element over a relatively broad frequency range of typically 500 Å, over which continuous tuning is to be accomplished by varying the acoustic frequency input to the acousto-optic filter element. The filter element, consisting of a birefringent nonlinear crystal and appropriate polarizers, discriminates against all frequencies that do not satisfy the phase-matching condition set by the acoustic frequency, while passing those frequencies within a narrow range (on the order of 1 Å, depending on the birefringence and length of the nonlinear crystal) that do phase match. It is also conceivable (by virtue of similarity to the FM laser case) that some particular mode of operation of the system may involve the generation of extremely short phase-locked pulses, whose frequency may be tuned as above. If phase-locking is not an inherent feature, it may be induced by introducing a phase-perturbing element driven at the axial mode frequency separation into the cavity, as with the FM laser. The generation of short tunable pulses would make this system an extremely useful device to spectroscopists and others.

The theory of the acousto-optic filter has been treated in a paper by S. E. Harris and R. W. Wallace,[2] and several versions of the filter have been successfully constructed by S. T. K. Nieh, the first of which

[2] S. E. Harris and R. W. Wallace, "Acousto-Optic Tunable Filter," J. Opt. Soc. Amer. 59, 744 (June 1969).

has been reported in a paper by S. E. Harris, S. T. K. Nieh, and D. K. Winslow.[3] We have been extending the theory of the acousto-optic element as it would be applied in the tunable dye laser, including certain complications that have not been covered in previous analyses. One of these complications is the consideration of acoustic standing waves, or equivalently, acoustic waves traveling collinearly both with and against the light waves. For an acoustic wave traveling in one direction only, say $+x$, the acousto-optic interaction causes diffraction of y polarized light (for a material with $n_e > n_0$) traveling in the $+x$ direction at frequency ω_0 into z polarized light at frequency $\omega_1 = \omega_0 + \omega_a$, where ω_a is the acoustic frequency, with cumulative diffraction resulting if the phase matching condition $\Delta k = k_{1z} - k_{0y} - k_a \approx 0$ is met; furthermore, there is no coupling of these waves to any other modes. The results of this analysis can be put in the form of Jones matrices of transmission. Assume interaction with an S_{13} shear wave through the p_{45} elasto-optic coefficient in a nonlinear crystal in Class 4/M (e.g., $CaMoO_4$). If we represent the fields (neglecting acoustic depletion) by

$$E_y(x,t) = \mathrm{Re}\left[\hat{E}_{0y}(x)\, e^{j(\omega_0 t - k_0 x)}\right]$$

$$E_z(x,t) = \mathrm{Re}\left[\hat{E}_{1z}(x)\, e^{j(\omega_1 t - k_1 x)}\right]$$

$$S_{13}(x,t) = \mathrm{Re}\left[\hat{S}_5\, e^{j(\omega_a t - k_a x)}\right]$$

[3] S. E. Harris, S. T. K. Nieh, and D. K. Winslow, "Electronically Tunable Acousto-Optic Filter," Appl. Phys. Letters 15, 10, 325-326 (15 November 1969).

then

$$\begin{bmatrix} \hat{E}_{0y}(x=L) \\ \\ \hat{E}_{1z}(x=L) \end{bmatrix} = \begin{bmatrix} a_{11} & a_{12} \\ \\ a_{21} & a_{22} \end{bmatrix} \begin{bmatrix} \hat{E}_{0y}(x=0) \\ \\ \hat{E}_{1z}(x=0) \end{bmatrix}.$$

where

$$a_{11} = e^{-j\frac{\Delta k}{2}L}\left\{\cos\left[\left(K_0^*K_1 + \frac{\Delta k^2}{4}\right)^{\frac{1}{2}} L\right] + j\,\frac{\Delta k}{2}\sin\left[\left(K_0^*K_1 + \frac{\Delta k^2}{4}\right)^{\frac{1}{2}} L\right]\Big/\left(K_0^*K_1 + \frac{\Delta k^2}{4}\right)^{\frac{1}{2}}\right\}$$

$$a_{12} = j\,e^{-j\frac{\Delta k}{2}L}\,K_0^*\sin\left[\left(K_0^*K_1 + \frac{\Delta k^2}{4}\right)^{\frac{1}{2}} L\right]\Big/\left(K_0^*K_1 + \frac{\Delta k^2}{4}\right)^{\frac{1}{2}}$$

$$a_{21} = j\,e^{j\frac{\Delta k}{2}L}\,K_1\sin\left[\left(K_0^*K_1 + \frac{\Delta k^2}{4}\right)^{\frac{1}{2}} L\right]\Big/\left(K_0^*K_1 + \frac{\Delta k^2}{4}\right)^{\frac{1}{2}}$$

$$a_{22} = e^{j\frac{\Delta k}{2}L}\left\{\cos\left[\left(K_0^*K_1 + \frac{\Delta k^2}{4}\right)^{\frac{1}{2}} L\right] - j\,\frac{\Delta k}{2}\sin\left[\left(K_0^*K_1 + \frac{\Delta k^2}{4}\right)^{\frac{1}{2}} L\right]\Big/\left(K_0^*K_1 + \frac{\Delta k^2}{4}\right)^{\frac{1}{2}}\right\}$$

where

$$\Delta k = k_1 - k_0 - k_a = \frac{\omega_1 n_e}{c} - \frac{\omega_0 n_0}{c}\,\frac{\omega_a}{v_a}$$

$$K_0^* = \frac{\omega_0}{2c}\,n_0 n_e^2\,p_{45}\,\hat{S}_5^*$$

$$K_1 = \frac{\omega_1}{2c}\,n_0^2 n_e\,p_{45}\,\hat{S}_5$$

Similar analyses can deal with other cases characterized by an acoustic wave traveling in one direction only.

The complication introduced by acoustic standing waves is coupling into higher-order modes. For example, if the diffraction of y-polarized light at ω_0 into z-polarized light at $\omega_1 = \omega_0 + \omega_a$ is nearly phase matched by a $+x$ traveling acoustic wave, then the diffraction of the z-polarized light at ω_1 into y-polarized light at $\omega_2 = \omega_1 + \omega_a$ is nearly phase matched by a $-x$ traveling acoustic wave, etc. This coupling limits the total diffraction efficiency from y-polarized light to z-polarized light to something considerably less than 100%, depending upon the relative amplitudes of the traveling acoustic waves; this effect has been experimentally confirmed by S. T. K. Nieh.[3] If the traveling acoustic waves are given by $S_{13}(x,t) = \mathrm{Re}\left[\hat{S}_+ e^{j(\omega_a t - k_a x)} + \hat{S}_- e^{j(\omega_a t + k_a x)}\right]$, the infinite set of coupled differential equations can be solved for the case $\hat{S}_+ = \hat{S}_+^* = \hat{S}_- = \hat{S}_-^* \equiv S$ if the phase-matching condition is satisfied, by noting their similarity to Bessel function recursion relations, giving the results (for incident light at ω_0 polarized along the y-axis)

$$E_y(x,t) = \mathrm{Re}\left[\sum_{n\ \mathrm{even}} \hat{E}_n(x)\, e^{j[\omega_n t - (n_0\omega_n/c)\,x]}\right]$$

$$E_z(x,t) = \mathrm{Re}\left[\sum_{n\ \mathrm{odd}} \hat{E}_n(x)\, e^{j[\omega_n t - (n_e\omega_n/c)\,x]}\right]$$

with $\omega_n = \omega_0 + n\omega_a$, $\hat{E}_n(x) = E_0(0)\, j^n J_n(\alpha x)$, where $\alpha = \omega_0 (n_0^3 n_e^3)^{\frac{1}{2}}\, p_{45} S/c$. If single-pass conversion efficiency η is defined by $\eta = \langle S^{(z)}(L,t)\rangle / \langle S^{(y)}(0,t)\rangle$

where $S^{(z)}$ denotes the power density carried by the z-polarized electric field, then

$$\eta = \frac{n_e}{n_0} \sum_{n \text{ odd}} J_n^2 (\alpha L) .$$

η reaches its first maximum for $\alpha L \approx 1.9$, with $\eta_{max} \approx 0.74$. Thus single-pass losses are $\geq 26\%$ for this particular choice of acoustic standing wave, emphasizing the point that acoustic standing waves should be avoided if this element is to be placed inside a dye laser cavity.

Another complication that we are considering involves the upward shift in frequency of the output light when 100% conversion is attained with an acoustic wave traveling in one direction. Furthermore, if this output light is reflected back into the acousto-optic element it can be 100% converted back into the original polarization, but with another upward shift in frequency. We are currently studying the significance of these frequency shifts to the operation of the laser by considering the fundamental concepts of cavity resonances. If these frequency shifts should prove detrimental, various schemes have been proposed to compensate for them.

Now that several versions of the acousto-optic filter, including a straight-through filter, have been successfully constructed, we plan to construct in the immediate future a straight-through acousto-optic element that can be placed inside an already existing flashlamp-excited dye laser. The nonlinear crystal to be used will be CaM_0O_4 , since this material has a low birefringence and hence requires relatively low acoustic frequencies (in the range of 50 MHz) to tune in the visible spectrum. Later work may include: construction of our own dye laser cavity; introduction of different nonlinear crystals (e.g., $LiNbO_3$, which will produce a much narrower output line than CaM_0O_4); and generation of short phase-locked pulses.

3. Laser Stabilization Studies (S. C. Wang)

The investigation of saturable absorption of DME (di-methyl-etha) gas with a He-Xe laser at 3.51μ is continuing. The observation of the output power spectrum shows several inverted Lamb dips which are due to saturation of absorption of DME gas. The frequency separation of these dips are a few MHz to a few tens of MHz . Each saturation peak has a width of about 1 MHz . Attempts to interpret this high resolution spectrum based on the molecular spectroscopy of DME have been started. However, due to the complex molecular structure of DME (an asymmetric top with internal rotors), the interpretation is very difficult. Qualitatively, the dips can be interpreted as contributions from internal rotation (which according to published microwave spectrum is a triplet with separation of MHz) and possible high-order effects such as interaction with vibration and rotation levels.

Work is also continuing to reduce the data in order to obtain other significant information about DME gas, such as absorption coefficient, cross-section, saturation power, and transition dipole moment. An absorption coefficient of 0.007 cm^{-1} and cross-section of about 6×10^{-15} cm^2 have been obtained to date.

From the results of this experiment on DME gas, we conclude that DME gas, although showing saturable absorption, is not a promising gas for frequency stabilization purposes due to its complicated molecular structure. However, the saturable absorption provides valuable information about the gas and the dynamics of the laser.

At present, we are modifying our experiment to use a pure Xe cell inside a He-Xe laser cavity. Using this setup we will investigate the second method of frequency stabilization and the enhanced Lamb dips of the saturation of the Xe gas cell. The Xe gas is known to have a linewidth of about 100 kHz so that this absorption peak should lead to the possibility of stabilizing the laser to one part in 10^{12}.

4. Backward Wave Oscillation (J. Falk and S. E. Harris)

This project is concerned with an attempt to produce a tunable source in the 1 millimeter region of the spectrum via a temporally unstable, "backward wave", three-photon interaction.

Previous unsuccessful attempts at this experiment have used $LiTaO_3$ as the nonlinear medium. Problems with the quality of available $LiTaO_3$ have forced us to consider the use of other materials.[4]

During the past quarter an attempt was made at achieving backward wave oscillation in 10 degree cut $LiNbO_3$. Ten degree cut $LiNbO_3$ should provide backward wave phase matching at a signal wavelength of about 2 mm, where the calculated absorption of $LiNbO_3$ is small (less than 0.20 cm^{-1}). Calculated threshold for the onset of temporal instability in the available 4 cm crystal of $LiNbO_3$ is 120 MW/cm^2. For pump intensities of twice threshold (240 MW/cm^2) calculated signal buildup times are of order of several nanoseconds.

We note that cutting of the $LiNbO_3$ at 10 degrees to the c axis introduces walk-off between the extraordinary pump wave normal and its Poynting vector. Because of this walk-off the high pump intensities necessary for nanosecond rise times must be achieved while a large beam size is maintained. Since our ruby laser can be run at power no greater than 2 MW, it is difficult to achieve such pumping densities.

Our first attempt at backward wave oscillation in ten degree cut $LiNbO_3$ used pump power densities only slightly above threshold such that the expected buildup times were of order of several tens of nanoseconds.

---

[4] Microwave Laboratory Report No. 1801, Stanford University, October 1969.

To compensate for the long buildup time we operated the laser in a fundamental pulse lengthened mode.[5] This was achieved with a KDP second harmonic generator internal to a cavity which had been designed for overcoupling of the second harmonic. Pump pulses from this pulse lengthened system were of order of 200 kW and were 200 nsec long.

The results of this backward wave oscillation attempt were inconclusive. A spectral examination of the fundamental pulse lengthened laser with a high resolution grating spectrometer showed that the laser ran in several spectral lines spaced about 1 Angstrom from one another. Such spectral impurity of the ruby would probably mask any backward wave oscillations which we had hoped to detect by observing the parametrically generated idler, which would be shifted several Angstroms from the ruby pump. Furthermore, examination of the ruby rod used in the laser for the backward wave attempt showed severe cracking internal to the ruby. Whether this cracking is a consequence of thermal stresses or is due to other unknown factors is not yet understood. It is also not understood if the ruby's spectral impurity is a consequence of its cracking.

During the next quarter backward wave experimentation will continue with the 10 degree cut $LiNbO_3$ using a ruby laser operated in the conventional Q-switched mode such that ruby spectral purity may be insured.

---

[5] Section 1, page 3 of this report.